

Synthesis, structures and luminescence properties of $N^{\wedge}C^{\wedge}N$ -coordinated platinum(II) complexes based on an anthracene core: a red shift and a twist[§]

*Emily A. Wood, Louise F. Gildea, Dmitry S. Yufit, and J. A. Gareth Williams**

Department of Chemistry, Durham University, Durham, DH1 3LE, UK.

*E-mail: j.a.g.williams@durham.ac.uk

[§] Invited contribution to the special edition of *Polyhedron* commemorating the life and career of Professor Malcolm L. H. Green and his innumerable contributions to organometallic chemistry.

Abstract

1,8-Bis(2-pyridyl)anthracene HL² is shown to act as a tridentate, N[^]C[^]N-coordinating ligand to platinum(II), undergoing metallation at position 9 of the anthracene. The structures of Pt(N[^]C[^]N-L²)Cl and of HL² have been determined by X-ray diffraction. The complex features two 6-membered chelate rings and an N-Pt-N bite angle of 178.16(7)°, close to the “ideal” value of 180°. The attainment of this angle necessitates not only a twisting of the pyridyl rings relative to the anthracene, but also a remarkable twisting distortion of the anthracene unit itself. The complex is isomeric with the previously reported Pt(d8qb)Cl {d8qb = 1,3-di(8-quinolyl)benzene}. A new derivative of the latter has been prepared, PtL³Cl, featuring methyl substituents in the central benzene ring *ortho* to the quinolines. Like PtL²Cl, its structure shows twisting of the coordinated heterocycles relative to the plane of the central aromatic ring. The Pt(II) complex PtL¹Cl of a related N[^]C[^]N-coordinating ligand featuring extended conjugation, benzo[1,2-h:5,4=h']diquinoline HL¹, has also been prepared following a previously described procedure. PtL¹Cl is brightly phosphorescent in deoxygenated solution at ambient temperature, in the red region of the spectrum. The impressive photoluminescence quantum yield of 0.30 and long emission lifetime of 38 μs are indicative of a rigid structure with little excited state distortion. In contrast, PtL²Cl shows no detectable emission, probably due to the distorted nature of the structure leading to rapid non-radiative decay of the excited state. This result contrasts with the weak red emission displayed by the isomeric Pt(d8qb)Cl and its dimethylated derivative PtL³Cl.

Keywords

Anthracene, platinum, tridentate ligand, luminescence, 6-membered chelate ring.

Introduction

The phosphorescence properties of organometallic platinum(II) complexes attract a great deal of research interest [1]. The large spin-orbit coupling associated with platinum can promote the formally forbidden emission of light from triplet excited states, a process that is facilitated by the presence of Pt–C bonds, with their high degree of covalency, as opposed to purely coordination character [2]. Such effects are also at work in organometallic compounds of many other metals, particularly d^6 metal ions such as Re(I), Ru(II), Rh(III), and Ir(III) [3]. But the square-planar geometries typically favoured by d^8 Pt(II) complexes permit face-to-face intermolecular interactions that are not open to pseudo-octahedral d^8 complexes, which may in turn lead to the formation of excimers or aggregates [4]. Numerous potential applications of phosphorescent platinum(II) complexes have been explored, for example, in chemosensing [5], bioimaging [6], and light-emitting diodes [7].

Cyclometallating ligands predominate in the most brightly emissive complexes, particularly those based on 2-phenylpyridine (ppy) [8]. The synergy of strong σ -donation (C–Pt bond) and the π -accepting nature of the heterocycle leads to a strong ligand field, keeping metal-centred d-d excited states to high energy and thus limiting both undesirable non-radiative decay and ligand photolability through the population of d orbitals with metal-ligand anti-bonding character [9]. Tridentate analogues [10], particularly those based on tridentate $N^2C^1N^1$ -coordinating ligands such as 1,3-di(2-pyridyl)benzene (dpyb) (Figure 1) [11], have proved particularly successful, owing in part to the higher rigidity of their complexes (*e.g.*, with respect to a D_{4h} to D_{2d} distortion), suppressing excited-state distortions that can contribute to non-radiative decay pathways [12]. Such distortions also have a beneficial effect on colour purity by reducing the contribution of higher vibrational components in the long-wavelength tail of the spectrum, a particularly desirable feature in the design of OLED emitters [*op. cit.*].

The most highly emissive metal complexes, with highest quantum yields, are green-emitting molecules. Red emitters tend to be display weaker emission, due in part to the effect of faster non-radiative decay of low-energy excited states through vibrational transfer (the so-called “energy gap law”) [13]. Yet, deep red and near-infra-red emitting complexes are of particular interest in, for example, biological and medical applications, owing to the greater transparency of biological tissue to light in the 700–1100 nm region of the spectrum [14]. While emission maxima ≥ 700 nm are well-established for bimolecular (aggregate or excimer) excited states of Pt(II) complexes [15], complexes with sufficient conjugation to emit in this region from monomolecular states in solution remain quite rare, being limited largely to platinum porphyrins and phthalocyanines and related molecules [16, 17].

In this contribution, we describe two new Pt(II) complexes of *N*[^]*C*[^]*N*-coordinating ligands that feature more extended conjugation based on an anthracene unit (Figure 1). These complexes were targeted with a view to exploring the extent to which their phosphorescence would be red-shifted compared to that of the archetypal complex Pt(dpyb)Cl. Whilst the sought after result was obtained in one case, the other gave a very different outcome.

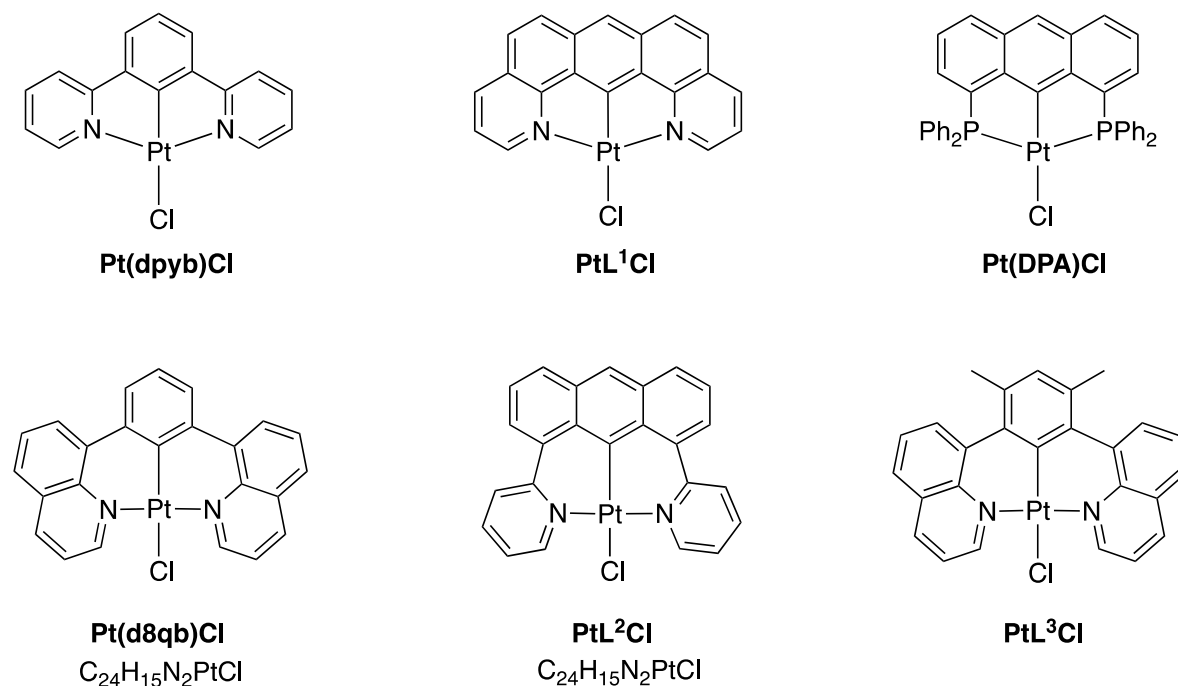


Figure 1 Structures of the new complexes PtL¹Cl, PtL²Cl, and PtL³Cl investigated in this work. Also shown are the structures of Pt(dpyb)Cl, the parent *N*[^]*C*[^]*N*-cyclometallated complex; Pt(d8qb)Cl, with which PtL²Cl is isomeric as seen from the molecular formulae; and Pt(DPA)Cl, a structurally related *P*[^]*C*[^]*P*-coordinated phosphine-based complex.

Results and Discussion

Rationale

Proligand HL¹, benzo[1,2-*h*: 5,4=*h'*]diquinoline (Figure 2), was reported in 2011 by Young *et al.* who showed that it can act as an *N*[^]*C*[^]*N*-coordinating ligand to M = Pd(II) and Pt(II), giving complexes of the form ML¹X (X = Cl or OAc) [18]. The resulting coordination is analogous to that of Pt(dpyb)Cl, with two 5-membered chelate rings being formed. Proligand HL², 1,8-di(2-pyridyl)anthracene, has not been reported previously. We reasoned that it should be able to act as an *N*[^]*C*[^]*N*-coordinating ligand, but it differs from dpyb and L¹ in that the resulting chelate rings will be 6-membered. Tridentate ligands binding in this way through 6-membered chelates can offer a more favourable bite angle at the metal, close to the ideal angle of 180°,

compared to angles typically of around 160° for more conventional ligands like terpyridine and its cyclometallating analogues that form 5-membered chelate rings [19]. In this respect, PtL^2Cl resembles $\text{Pt}(\text{d8qb})\text{Cl}$ (Figure 1) whose synthesis and photophysical properties we reported previously [20]. In fact, the two complexes are isomers of one another, and thus it was particularly interesting to explore how their emission properties would compare.

Synthesis of proligands and complexes

The preparation of HL^1 was carried out by means of a modified Skraup procedure, in which 1,8-diaminoanthracene was subjected to a double cyclization with acrolein formed *in situ* from glycerol, using a procedure based on that of Young *et al.* [18] but employing sodium sulfide for the initial reduction which gave improved results over SnCl_2 (Figure 2a). The desired platinum(II) complex PtL^1Cl was obtained as an orange solid upon reaction of HL^1 with K_2PtCl_4 in acetic acid. The identity of the complex was confirmed by a combination of ^1H and ^{13}C NMR spectroscopy and mass spectrometry. Cyclometallation is accompanied by the loss of a characteristic high-frequency resonance at 11.24 ppm in the uncoordinated ligand (corresponding to the H^9 position of the anthracene unit) and the appearance of ^{195}Pt satellites for the quinoline protons *ortho* to the coordinated nitrogen atoms, with a coupling constant of 42 Hz. Although we have not been able to obtain a crystal structure of this complex, Young *et al.* reported the structure of the corresponding Pd(II) complex, which showed the $N^{\wedge}C^{\wedge}N$ -coordinated metal ion sitting in the plane of the ligand, as expected. The Pt(II) complex is expected to have a similar structure.

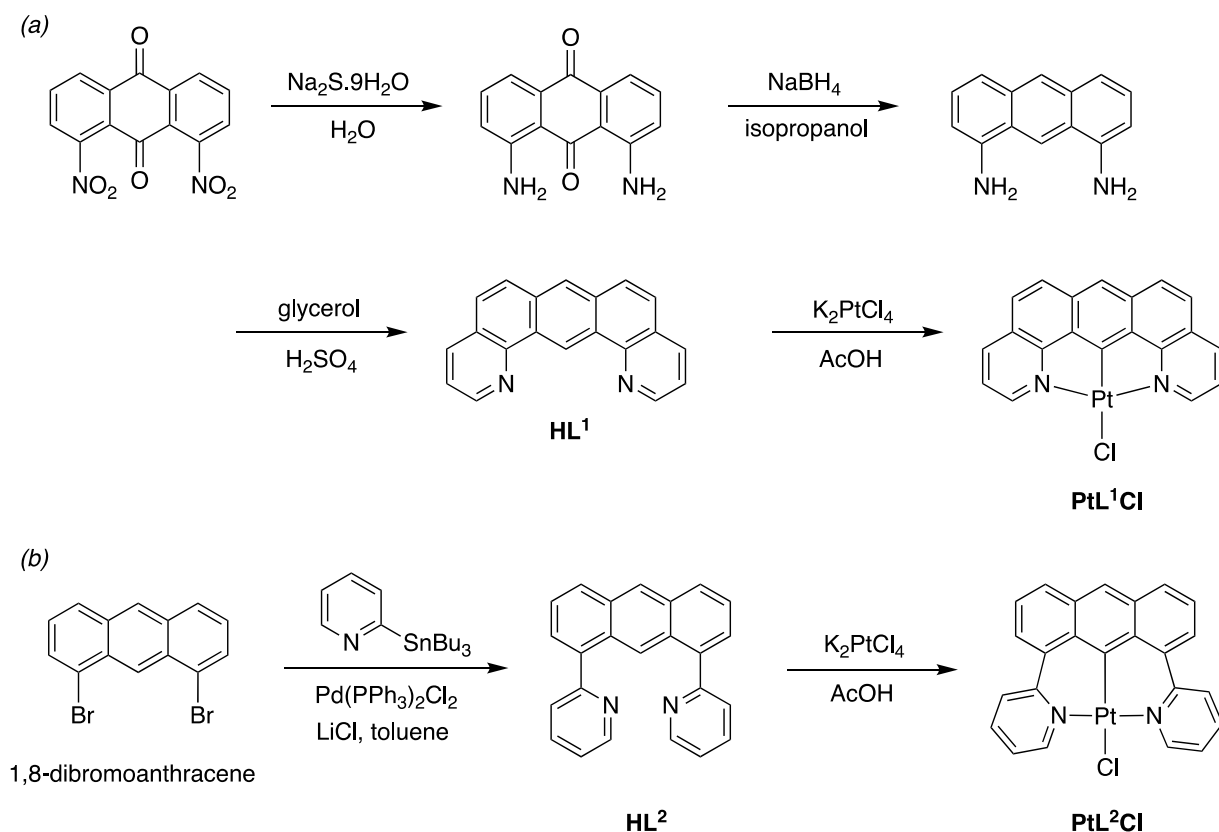


Figure 2 Synthetic routes to HL¹, HL² and their respective Pt(II) complexes

In order to prepare the new proligand HL², we selected a route involving a palladium-catalysed Stille coupling of 1,8-dibromoanthracene with 2-(tri-*n*-butylstannyl)pyridine in toluene (Figure 2b). The desired product was isolated in 41% yield after purification by column chromatography followed by recrystallization. Crystals suitable for study by X-ray diffraction were obtained upon cooling of a solution in hot ethanol. The structure (Figure 3) shows a planar anthracene unit and the pyridine rings twisted out of the plane, with torsion angles of 48.4(2)° and 47.5(2)°. One of the pyridyl rings is disordered over two positions, related through a 180° rotation about the C9–C20 bond. There are π - π and C–H \cdots π stacking interactions between adjacent molecules in the crystal.

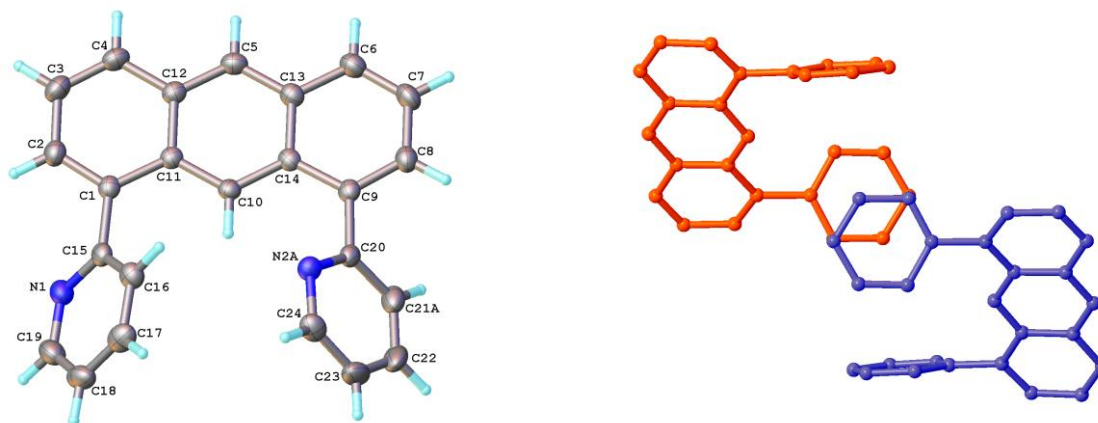


Figure 3 Molecular structure of HL² (left) and the π - π interactions between molecules in the crystal (right). Selected torsion angles: C2-C1-C15-N1 = 48.4(2) $^\circ$; C14-C9-C20-N2A = -47.5(2) $^\circ$.

The platination of HL² was achieved by reaction with K₂PtCl₄ in AcOH at reflux for 75 h. After separation of a brown precipitate, the desired complex was isolated as an orange-red solid by allowing the filtrate to crystallise over a period of 4 days. Evidence for the desired N[^]C[^]N coordination mode is provided by the ¹H NMR spectrum, with the loss of signal corresponding to H⁹ of the anthracene unit and a substantial downfield shift of the H⁶ resonances from 8.73 to 9.91 ppm. The identity of PtL²Cl was unequivocally confirmed by X-ray diffraction of crystals obtained from a solution in dichloromethane / hexane. The structure (Figure 4) shows the Pt(II) centre bound in a square planar geometry to the N[^]C[^]N-coordinated ligand, with the coordination sphere completed by a chloride ligand. The most remarkable feature, however, is the extraordinary distortion of the anthracene unit itself, with maximal torsion angles around central C11–C12 and C13–C14 bonds of 19.5(3) and 20.1(3) $^\circ$ respectively. At the same time, in order to accommodate the planar conformation at Pt(II), the pyridyl rings are less twisted relative to the anthracene core than in the proligand, with torsion angles around C1–C15 and C20–C9 bonds less than 30 $^\circ$. The pyridyl rings are almost perpendicular to each other with a dihedral angle of 78.21(3) $^\circ$ between their planes. The result

is that the *trans*-N1-Pt-N2 angle is almost exactly 180°, as had been sought, compared to significantly smaller angles in related complexes comprising 5-membered chelates; *e.g.*, the corresponding angle in Pt(dpyb)Cl is 161.1(3)°. On the other hand, the Pt–C bond of 1.976(2) Å is significantly longer than that of 1.903(4) Å in Pt(dpyb)Cl. In terms of the packing of molecules in the crystal, $\pi\cdots\pi$ interactions between pyridine rings of adjacent molecules lead to chains along the [101] direction. Weak CH \cdots Cl and CH \cdots π contacts between chains combine them into a 3D-framework.

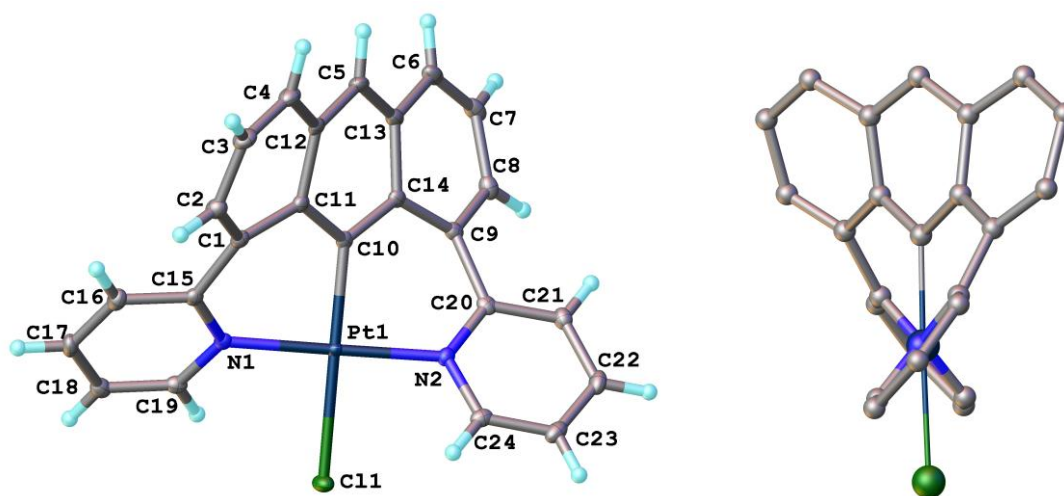


Figure 4 The molecular structure of PtL²Cl in the crystal and a view along the N-Pt-N line.

Selected bond lengths (Å) and angles (°): Pt1–C10 1.976(2), Pt1–N1 2.021(2), Pt1–N2 2.013(2), Pt1–Cl1 2.429(1); N1–Pt1–Cl1 90.94(5), N2–Pt1–Cl1 89.91(5), N2–Pt1–N1 178.16(7), C10–Pt1–Cl1 178.58(6), C10–Pt1–N1 89.60(8), C10–Pt1–N2 89.59(8).

The twisted orientation of the pyridyl rings relative to the plane of the central ligating unit is to be anticipated for ligands that form 6-membered chelate rings with large metal ions like Pt(II), as opposed to the more commonly encountered 5-membered ones [19]. A similar structure was previously postulated for Pt(b8qb)Cl, supported by DFT calculations [20], though no experimental structure has hitherto been available. In the current work, we prepared the corresponding complex of a derivative of d8qb, namely di(8-quinolyl)-*meta*-xylene (HL³), in the hope of obtaining crystals suitable for X-ray diffraction. This ligand features methyl

substituents in the central aryl ring *ortho* to the quinolines (Figure 5). Suitable crystals of PtL^3Cl were obtained. The resulting structure (Figure 6a,b) shows the twisting of the rings that had been predicted and a *trans*-N1-Pt-N2 angle of $177.8(2)^\circ$, *i.e.*, close to 180° and similar to that of PtL^2Cl . The twist of the heterocyclic arms is again clear, and can be compared with a structure of the uncoordinated proligand d8qb also obtained during the current work (Figure 6c). It is interesting to note that the complex has C_2 symmetry and thus comprises a racemic mixture of enantiomers. The crystal structure of PtL^3Cl does not contain any close contacts between parallel aromatic rings. The only noticeable direction-specific intermolecular interactions are of $\text{CH}\cdots\text{Cl}$ type.

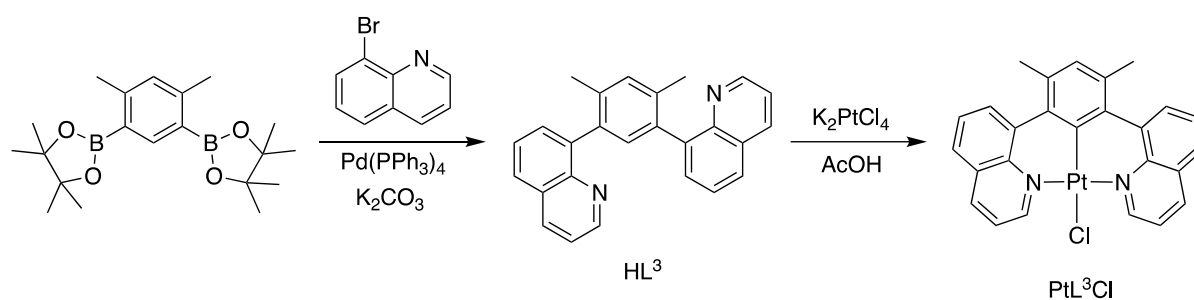


Figure 5 Synthesis of HL^3 and PtL^3Cl .

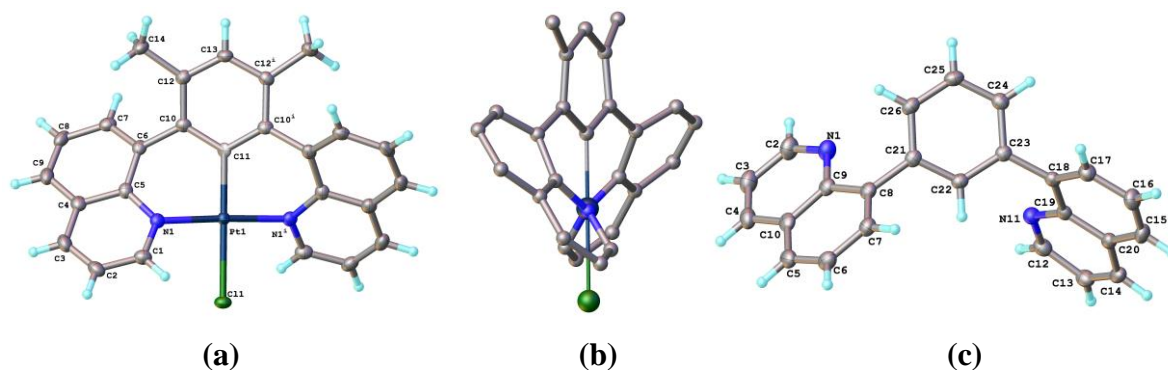


Figure 6 The molecular structure of PtL^3Cl in the crystal (a), viewed along the N-Pt-N line (b), and of the free d8qb ligand (c). The complex is located on a 2-fold axis (symm. code $i = 1-x, y, \frac{1}{2}-z$). Selected bond lengths (\AA) and angles ($^\circ$): Pt–C22 1.992(5), Pt–N1 2.035(3), Pt–Cl1 2.451(1); N1–Pt–N11 177.8(2), C22–Pt–C1 180.0.

A ligand ostensibly related to HL^2 , carrying PPh_2 phosphine ligating units at the 1,8 positions of anthracene, was previously used by Yip and co-workers to generate $\text{Pt}(\text{DPA})\text{Cl}$ {DPA = 1,8-bis(diphenylphosphino)anthracene} (Figure 1) [21]. It may be noticed, however, that the chelate rings which form in that case are 5-membered: the resulting structure shows a correspondingly more acute P–Pt–P angle of $167.34(3)^\circ$. Indeed, the structure of that ligand and complex are arguably more similar to PtL^1Cl , the phosphorus donors being in the positions corresponding to the nitrogen atoms of the conjugated system of L^1 .

Photophysical properties

The absorption spectrum of PtL^1Cl in dichloromethane solution at room temperature (Figure 7a) shows very intense bands in the UV region, attributable to ligand-based $\pi\text{-}\pi^*$ transitions, accompanied by intense ones in the visible region with maxima at 433 and 462 nm. The separation of this pair of bands (1450 cm^{-1}) is consistent with the first and second components of a vibrational progression corresponding to aromatic C=C stretches. The proligand HL^2 has no absorption in the visible region, but shows a vibrational progression in the UV with $\lambda(0,0) =$

394 nm. Such a set of bands is quite typical of polycyclic aromatics, corresponding to the vibrational components of the lowest spin-allowed intraligand π - π^* transition. The large red shift observed on going from the proligand to the complex (around 3700 cm^{-1}) is most likely due to introduction of significant charge-transfer character associated with cyclometallation, leading to transitions of mixed intraligand and metal-to-ligand charge-transfer ($d_{\text{Pt}} | \pi_{\text{L}} \rightarrow \pi_{\text{L}}^*$) character, by analogy with studies of related cyclometallated complexes [22]. The spectrum of PtL^2Cl under the same conditions is fairly similar to PtL^1Cl , although the bands in the visible region are red-shifted by around 40 nm (to 474 and 502 nm) whilst the bands in the UV region are less well-resolved (Figure 7b). The red shift relative to the corresponding proligand (HL^2) is even larger in this instance, around 5600 cm^{-1} .

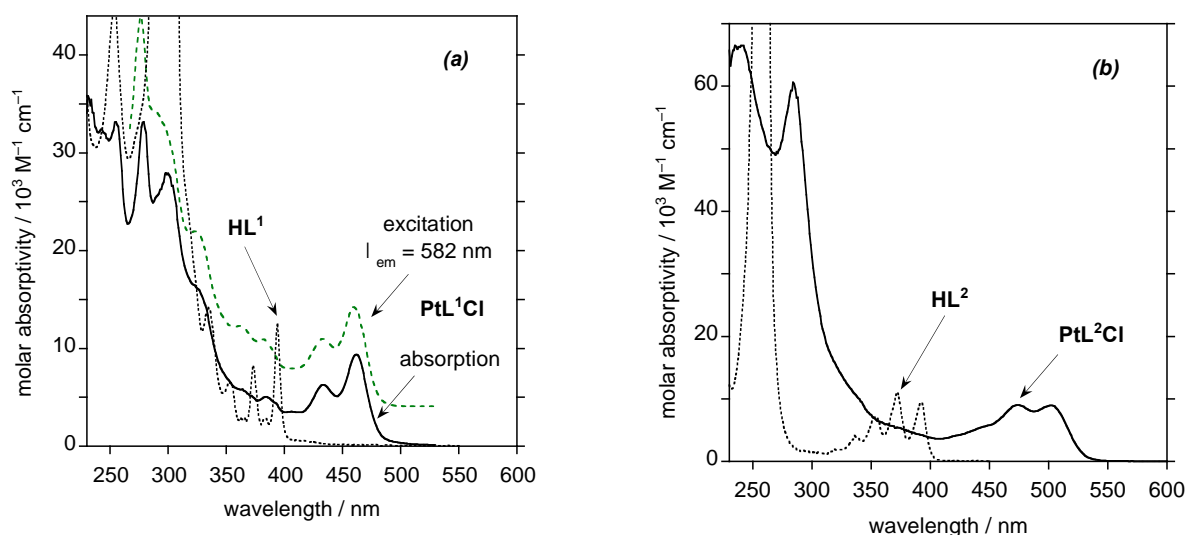


Figure 7 The absorption spectra of (a) PtL^1Cl and HL^1 (solid and dotted lines respectively), and (b) PtL^2Cl and HL^2 (solid and dotted lines respectively), in CH_2Cl_2 at $295 \pm 1\text{ K}$. The photoluminescence excitation spectrum of PtL^1Cl under the same conditions, registered at $\lambda_{\text{em}} = 582\text{ nm}$, is also shown by the green dashed line in (a).

The complex PtL^1Cl is intensely luminescent in deoxygenated solution at ambient temperature, in the deep orange-to-red region. The emission spectrum shows a well-resolved vibrational progression of around 1400 cm^{-1} , with the 0,0 band at 582 nm being the most intense

component (Figure 8). The photoluminescence quantum yield under these conditions is 0.30, and the emission decay follows monoexponential kinetics with a lifetime of 38 μs . Not surprisingly, given the long lifetime, the emission is strongly quenched by dissolved molecular oxygen, with the lifetime being shortened to 570 ns in air-equilibrated solution.

The impressive quantum yield compares favourably with many mononuclear Pt(II) complexes, where emission efficiency tends to fall on moving to the red as vibrational decay increases. Meanwhile, the lifetime is unusually long, even for brightly emitting Pt(II) complexes. Some insight into these emission properties can be obtained by estimating the radiative and non-radiative decay rate constants, k_r and Σk_{nr} respectively, according to the equations $k_r = \Phi / \tau$ and $k_{nr} = (1-\Phi) / \tau$. These relationships hold if the emitting state is formed with unit efficiency, and it is clear from the close match between the photoluminescence excitation spectrum registered at $\lambda_{em} = 582$ nm and the absorption spectrum (Figure 5a) that such an approximation is appropriate here. The value of k_r so obtained (7900 s^{-1}) is an order of magnitude lower than for Pt(dpyb)Cl [11a] but non-radiative decay k_{nr} (18000 s^{-1}) is also reduced by a factor of 3, such that the emission is long-lived yet remains intense. The reduced value of k_r may reflect a diminishing contribution of metal character to the excited state, as the extent of conjugation in the ligand increases and the highest filled ligand-based orbitals rise in energy [23]. The emissive excited state is thus probably more $\pi-\pi^*$ in nature, as opposed to featuring high MLCT character (typical of complexes with fast radiative decay like *fac*-Ir(ppy)₃ for example). On the other hand, the attenuated rate of non-radiative decay may be a reflection of the highly rigid nature of the complex. At 77 K, the vibrational structure becomes further resolved, but the shift of the emission bands to higher energy is barely perceptible, behaviour that is again indicative of a highly rigid system with little excited state distortion occurring at room temperature. The lifetime at 77 K is lengthened to 58 μs .

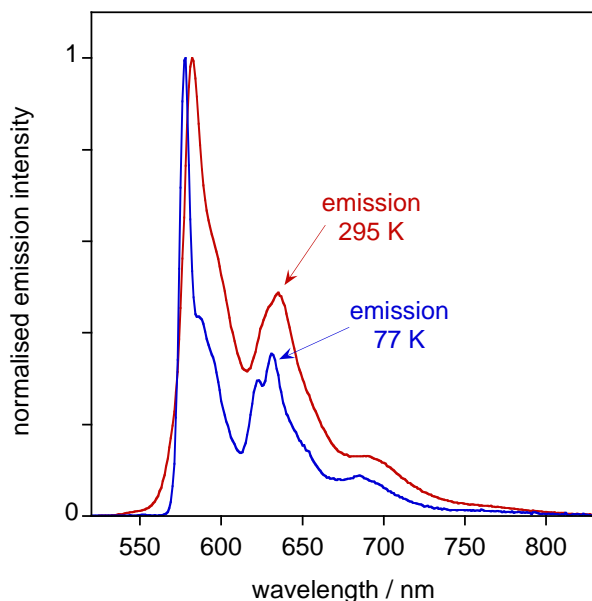


Figure 8 The photoluminescence spectra of PtL^1Cl in CH_2Cl_2 at 295 K (red) and in EPA at 77 K (EPA = diethyl ether / isopentane / ethanol: 2:2:1 v/v).

The complex PtL^2Cl , in contrast, displays no detectable emission at ambient temperature. Even in a frozen glass at 77 K, we were unable to record a convincing spectrum. Thus, it appears that the highly distorted nature of the anthracene core permits fast non-radiative decay that competes too effectively for emission to be observed. The phosphine complex $\text{Pt}(\text{DPA})\text{Cl}$ reported by Yip and co-workers (Figure 1) displayed very different photophysical properties, with bright blue emission centred at 474 nm [21]. Most likely, the emission in that case is fluorescence from a singlet state localised on the anthracene [24].

Our previously investigated $\text{Pt}(\text{d8qb})\text{Cl}$ complex, with which PtL^2Cl is isomeric, is phosphorescent in the red region but has a much lower quantum yield (0.016) than PtL^1Cl [20]. Similarly, the newly prepared complex PtL^3Cl of the current work displays emission spectra at 295K and at 77K that are essentially identical to those of $\text{Pt}(\text{d8qb})\text{Cl}$ [20]. The quantum yield and lifetime are marginally reduced, though the difference is barely greater than the uncertainty

in the measurements $\{\Phi = 0.014 \text{ and } 0.016, \tau = 10 \text{ and } 14 \mu\text{s}, \text{ for PtL}^3\text{Cl and Pt(d8qb)Cl respectively}\}$. This illustrates that the flanking methyl groups evidently have little steric effect on the structure of PtL³Cl compared to the parent, owing to the intrinsic twisting of the planes of the pyridyl rings that occurs for these ligands upon binding to the metal. In contrast, in diimine and triimine ligands that bind through 5-membered chelates, like bipyridine and terpyridine, such flanking methyl substituents typically have a detrimental effect on emission efficiencies of their complexes, since the ensuing twist compromises the ligand field strength [25].

Conclusions

In summary, both benzodiquinoline HL¹ and 1,8-di(2-pyridyl)anthracene HL² are able to function as *N*[^]*C*[^]*N*-cyclometallating ligands through deprotonation of the C–H unit between the ligating nitrogen atoms, forming two 5-membered chelate rings and two 6-membered chelate rings respectively. The Pt(II) complex of the former, PtL¹Cl, turns out to be a bright red phosphor in deoxygenated solution with an unusually long decay time of 38 μs , in part reflecting a lowered rate of non-radiative decay associated with the highly rigid structure. Coupled with the respectable quantum yield of 0.30 under these conditions, these properties render it potentially suited to applications as a triplet sensitiser or oxygen sensor, for example. In contrast, PtL²Cl is non-emissive, and its structure shows an unusual distortion of the anthracene core. The pyridyl rings are twisted relative to one another, a feature previously postulated – and now confirmed here structurally – also for complexes of di(8-quinolyl)benzene ligands that similarly bind through the formation of two 6-membered rings.

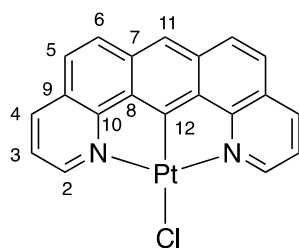
Experimental

Synthetic details and characterisation of compounds

^1H and ^{13}C NMR spectra were recorded on a Bruker Avance-400 spectrometer or a Varian VNMRS-700. Chemical shifts (δ) are in ppm, referenced to residual protio-solvent resonances, and coupling constants are given in Hertz. Mass spectra were obtained by electrospray ionisation (positive and negative ionisation modes) on a Waters TQD mass spectrometer interfaced with an Acquity UPLC system with acetonitrile as the carrier solvent. Measurements requiring the use of an atmospheric solids analysis probe (ASAP) for ionisation were performed on Waters Xevo QToF mass spectrometer.

Ligand HL¹ was prepared from 1,8-diaminoanthracene using the sequence of reactions described by Young *et al.* [18]. In that work, the requisite 1,8-diaminoanthracene was prepared from 1,8-dichloroanthraquinone via the intermediacy of a sulfonamide prepared by copper-catalysed substitution of the halogens with *para*-toluenesulfonamide. In our hands, that procedure gave poor results. We therefore turned to an alternative route involving the stepwise reduction of 1,8-dinitroanthraquinone, first of the nitro groups using sodium sulfide {as described for related anthraquinones by Ghaieni *et al.* [26] and which gave higher yields than the use of tin(II) chloride} and then of the carbonyl units using NaBH₄.

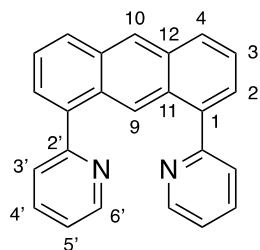
PtL¹Cl



A mixture of HL¹ (10 mg, 0.036 mmol), K₂PtCl₄ (17.8 mg, 0.043 mmol) and glacial acetic acid (3.2 mL) in a Schlenk was degassed via three freeze-pump-thaw cycles and then refluxed under an argon atmosphere for 120 h. The orange-brown precipitate that formed was washed successively with water, methanol and diethyl ether (2 × 3 mL of each) and then dried. Further washing with portions of CH₂Cl₂ followed by centrifugation gave the desired product as an orange solid (11.8 mg, 64%). ^1H NMR (CDCl₃, 400 MHz): $\delta_{\text{H}} = 9.29$ (2H, dd, J 5.5, J 1.0

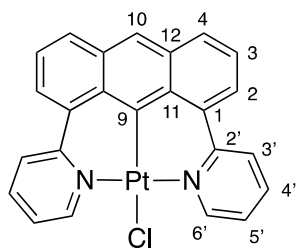
with coupling to ^{195}Pt , H^2), 8.43 (2H, dd, J 8.0, J 1.0, H^4), 8.09 (1H, s, H^{11}), 7.98 (2H, d, J 9.0, H^6), 7.74 (2H, d, J 9.0, H^5), 7.63 (2H, dd, J 8.0, J 5.5, H^3). ^{13}C NMR (CDCl_3 , 176 MHz): δ_{C} = 166.6 (C^{12}), 160.9 (C^{10}), 151. (C^2), 136.9 (C^4), 133.6 (C^8), 133.1 (C^7), 129.1 (C^6), 126.9 (C^9), 126.2 (C^5), 122.4 (C^3), 113.7 (C^{11}). MS (ASAP+): m/z = 514 $[\text{M}-\text{Cl}+\text{MeCN}]^+$. HRMS (ASAP+): m/z = 514.0829 $[\text{M}-\text{Cl}+\text{MeCN}]^+$, calculated for $[\text{C}_{22}\text{H}_{14}\text{N}_3^{194}\text{Pt}]^+ = 514.0815$.

1,8-Dipyridylanthracene HL²



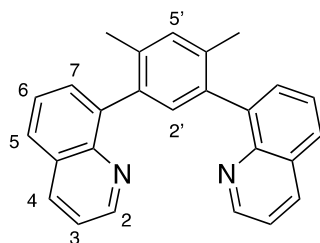
A mixture of 1,8-dibromoanthracene (200 mg, 0.60 mmol), 2-(tributylstannyl)pyridine (555 mg, 1.49 mmol), LiCl (202 mg, 4.76 mmol) and dry toluene (8 mL) in a Schlenk was degassed via three freeze-pump-thaw cycles and then back-filled with argon. The catalyst $\text{PdCl}_2(\text{PPh}_3)_2$ (33 mg, 0.048 mmol) was added under a flow of argon and the mixture was refluxed at 110°C for 48 h, after which a further portion of 2-(tributylstannyl)pyridine (114 mg) was added and heating sustained for a further 20 h. Upon cooling to room temperature, saturated aqueous KF solution (5 mL) was added; the mixture was stirred for 30 minutes and then filtered. The solvent was removed from the filtrate under reduced pressure; CH_2Cl_2 (40 mL) was added, and the resulting solution washed with NaHCO_3 (5 wt%, 3 x 20 mL) and then dried over anhydrous K_2CO_3 . The product was purified by column chromatography on silica (hexane: ethyl acetate, 30:70, $R_f = 0.49$). Further purification via recrystallisation from ethanol gave the desired product as small yellow crystals (81 mg, 41% yield). ^1H NMR (CDCl_3 , 400 MHz): δ_{H} = 9.03 (1H, s, H^9), 8.73 (2H, ddd, J 5.0, J 2.0, J 1.0, $\text{H}^{6'}$), 8.57 (1H, s, H^{10}), 8.10 (2H, d, J 8.5, H^4), 7.80 (2H, td, J 7.5, J 2.0, H^4), 7.68 (2H, d, J 8.0, H^3), 7.65 (2H, dd, J 7.0, J 1.0, H^2) 7.57 (2H, dd, J 8.5, J 7.0, H^3) 7.30 (2H, ddd, J 7.5, J 5.0, J 1.0 $\text{H}^{5'}$). ^{13}C NMR (CDCl_3 , 150 MHz): δ_{C} = 159.0 (C^2), 149.3 ($\text{C}^{6'}$), 138.6 (C^1), 136.1 (C^4), 131.9 (C^{12}), 129.6 (C^{11}), 129.0 (C^4), 127.1 (C^2), 126.9 (C^{10}), 125.3 ($\text{C}^{3'}$), 125.1 (C^3), 123.3 (C^9), 121.9 (C^5). MS (ASAP+) m/z = 333 $[\text{M}+\text{H}]^+$. HRMS (ASAP+) m/z = 333.1379 $[\text{M}+\text{H}]^+$, calculated for $[\text{C}_{24}\text{H}_{17}\text{N}_2]^+ = 333.1392$.

PtL²Cl



A mixture of HL² (18mg, 0.054 mmol), K₂PtCl₄ (27 mg, 0.065 mmol) and glacial acetic acid (5.7 mL) in a Schlenk was degassed via three freeze-pump-thaw cycles. The reaction mixture was refluxed under argon atmosphere for 120 h. The mixture was then centrifuged to yield a yellow solution and a brown solid. The desired product was slowly crystallised from the solution as bright orange crystals (13 mg, 43%). The complex shows some evidence of instability in solution. We note that anthracene-based metal complexes may sensitise and subsequently react irreversibly with singlet oxygen [21, 27], though no definitive products could be characterised in this instance. ¹H NMR (CDCl₃, 400 MHz): $\delta_{\text{H}} = 9.91$ (2H, dd, J 6.0, J 1.5 with coupling to ¹⁹⁵Pt, H^{6'}), 8.29 (2H, d, J 7.0, H⁴), 8.15 (1H, s, H¹⁰), 8.03 (2H, d, J 8.0, H²), 7.83 (4H, m, H^{3'}, H^{4'}), 7.43 (2H, dd, J 8.0, J 7.0, H³), 7.01-7.05 (2H, m, H^{5'}). ¹³C NMR (CDCl₃, 176 MHz): $\delta_{\text{C}} = 156.0$ (C^{6'}), 153.2 (C^{2'}), 152.8 (C⁹), 137.3 (C^{3'}), 137.0 (C¹), 131.8 (C²), 130.8 (C¹²) 126.4 (C¹¹), 125.2 (C^{4'}), 125.2 (C³), 123.9 (C⁴), 121.4 (C^{5'}), 121.1 (C¹⁰). MS (ES+) m/z : 525 [M-Cl]⁺. HRMS (ES+) $m/z = 525.0881$ [M-Cl]⁺, calculated for [C₂₄H₁₅N₂¹⁹⁴Pt]⁺ = 525.0862.

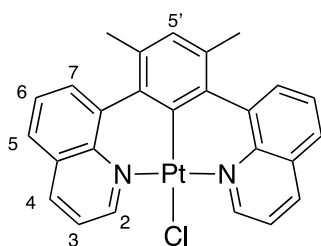
1,3-Bis(8-quinoly)-4,6-dimethylbenzene HL³



8-Bromoquinoline (116 mg, 0.56 mmol), 1,3-bis(pinacolatoboron)-4,6-dimethylbenzene (100 mg, 0.28 mmol) and Na₂CO₃ (645 mg) were combined in a mixture of ethanol (6 mL), toluene (6 mL) and water (3 mL). The mixture was degassed via four freeze-pump-thaw cycles, back-filled with nitrogen, and Pd(PPh₃)₄ (30 mg, 0.026 mmol) added under a positive pressure of nitrogen. The suspension was heated at reflux for 72 h. Upon cooling, water (5 mL) was

added and the product was extracted into CH₂Cl₂ (3 x 35 mL). The combined extracts were dried over anhydrous K₂CO₃, filtered and the solvent removed under reduced pressure to give a light brown oil. It was purified by column chromatography on silica (gradient elution from hexane to 65% hexane / 35% diethyl ether) to give HL³ as a colourless oil (59 mg, 58%). ¹H NMR (CDCl₃, 400 MHz) δ_H = 8.83 (2H, m, H²), 8.18 (2H, d, *J* 8.0, H⁴), 7.81 (2H, d, *J* = 8.0), 7.69 (2H, dd, *J* 7.0, 1.5), 7.53–7.57 (2H, m), 7.32–7.39 (2H, m), 7.18–7.27 (2H, m). MS (ES⁺) *m/z* = 361.2 [M + H]⁺. HRMS (ES⁺): *m/z* = 361.1704 [M + H]⁺, calculated for C₂₆H₂₁N₂ = 361.1705.

PtL³Cl



Solutions of HL³ (50 mg, 0.14 mmol) in acetonitrile (3 mL) and K₂PtCl₄ (75 mg, 0.18 mmol) in water (1 mL) were separately degassed via four freeze-pump-thaw cycles and then back-filled with nitrogen. The solution was heated at reflux under nitrogen for 72 h. The precipitate that formed was washed successively methanol, water, ethanol and diethyl ether (3 x 5 mL in each case). The residue was extracted into CH₂Cl₂ and the solvent then removed under reduced pressure to give the desired complex as a yellow solid (35 mg, 43%). ¹H NMR (CDCl₃, 700 MHz): δ_H = 9.47 (2H, d, *J* 5.0, H²), 8.37 (2H, d, *J* 7.5, H⁴), 8.04 (2H, d, *J* 7.0, H⁵ or H⁷), 7.79 (2H, d, *J* 8.5, H⁵ or H⁷), 7.64 (2H, t, *J* 7.5, H⁶), 7.31 (2H, dd, *J* 8.0, *J* = 5.0, H³), 7.13 (1H, s, H^{5'}). ¹³C NMR (CDCl₃, 176 MHz): δ_C = 155.6 (C²), 148.3 (q), 145.1 (q), 140 (q), 139.5 (C_q), 138.0 (C⁴), 134.1 (C^{5'} or q), 134.1 (q or C^{5'}), 132.2 (C⁵ or C⁷), 128.8 (q), 126.5 (C⁶), 125.7 (C⁷ or C⁵), 120.9 (C³), 24.1 (CH₃). MS (ASAP⁺) *m/z* = 590.09 [M + H]⁺. HRMS (ASAP⁺): *m/z* = 588.0864 [M]⁺, calculated for C₂₆H₁₉ClN₂¹⁹⁴Pt = 588.0864.

X-ray crystallography

The X-ray single crystal data have been collected using λMoKα radiation (λ = 0.71073 Å) on a Bruker D8Venture (Photon100 CMOS detector, IμS-microsource, focusing mirrors; compound PtL²Cl), Bruker SMART (CCD 1K detector, fine-focus sealed tube, graphite monochromator; compound d8qb), Bruker SMART (CCD 6000 detector, fine-focus sealed tube, graphite monochromator; compound PtL³Cl) and Agilent XCalibur (Sapphire-3 CCD detector, fine-

focus sealed tube, graphite monochromator, compound HL²) diffractometers equipped with a Cryostream (Oxford Cryosystems) open-flow nitrogen cryostats at temperature 120.0(2)K. All structures were solved by direct method and refined by full-matrix least squares on F² for all data using Olex2 [28] and SHELXTL [29] software. All non-hydrogen atoms were refined in anisotropic approximation; hydrogen atoms were placed in the calculated positions and refined in riding mode. Positional and vibrational parameters of N/C disordered atoms in one of the pyridyl rings in structure HL² were restricted to be the same, the SOF were refined to 0.52:0.48 values. Crystal data and parameters of refinement are listed in Table 1. Crystallographic data for the structures have been deposited with the Cambridge Crystallographic Data Centre as supplementary publication CCDC 2085961-2085964.

Table 1. Crystal data and structure refinement parameters

Compound	HL ²	PtL ² Cl	PtL ³ Cl	d8qb
Empirical formula	C ₂₄ H ₁₆ N ₂	C ₂₄ H ₁₅ ClN ₂ Pt	C ₂₆ H ₁₉ ClN ₂ Pt	C ₂₄ H ₁₆ N ₂
Formula weight	332.39	561.92	589.97	332.39
Temperature/K	120.0	120.0	120(2) K	120.0
Crystal system	Monoclinic	Triclinic	Orthorhombic	Orthorhombic
Space group	P2 ₁ /n	P-1	Pbcn	Pbca
a/Å	10.6084(3)	7.5150(8)	14.8633(4)	12.2613(10)
b/Å	8.9457(3)	10.5569(10)	13.6416(4)	10.4430(8)
c/Å	17.9717(5)	12.9057(13)	9.5078(3)	26.645(2)
α/°	90.00	66.383(3)	90.00	90.00
β/°	96.489(3)	88.500(3)	90.00	90.00
γ/°	90.00	72.624(3)	90.00	90.00
Volume/Å ³	1694.59(9)	890.18(16)	1927.79(10)	3411.7(5)
Z	4	2	4	8
ρ _{calc} /cm ³	1.303	2.096	2.033	1.294
μ/mm ⁻¹	0.077	8.044	7.434	0.076
F(000)	696.0	536.0	1136	1392.0
Crystal size/mm ³	0.35×0.21×0.04	0.14×0.1×0.01	0.28×0.26×0.04	0.5×0.1×0.03
Reflections collected	28203	19497	12194	27666
Independent refl., R _{int}	4945, 0.0719	5193, 0.0295	1972, 0.0400	3004, 0.0641
Data/restraints/parameters	4945/0/235	5193/0/253	1972 / 0 / 139	3004/0/235
Goodness-of-fit on F ²	1.039	1.091	1.028	1.100

Final R ₁ [$I \geq 2\sigma$ (I)]	0.0536	0.0168	0.0201	0.0435
Final wR ₂ [all data]	0.1332	0.0370	0.0565	0.0966
Diff. peak/hole / e Å ⁻³	0.27/-0.24	1.01/-0.92	2.163/0.830	0.15/-0.21

Solution-state photophysics

UV-visible absorption spectra were recorded on a Biotek Instruments Uvikon XS spectrometer operating with LabPower software. Emission spectra were acquired on a Jobin Yvon Spex Fluoromax-2 spectrometer. All samples were contained within 1 cm pathlength quartz cuvettes modified for connection to a vacuum line. Degassing was achieved by three freeze-pump-thaw cycles whilst connected to the vacuum manifold: final vapour pressure at 77 K was $< 5 \times 10^{-2}$ mbar. Emission was recorded at 90° to the excitation source, and spectra were corrected after acquisition for dark count and for the spectral response of the detector. The quantum yields were determined relative to an aqueous solution of [Ru(bpy)₃]Cl₃, for which $\Phi_{\text{lum}} = 0.040$.³⁰ Spectra at 77K were acquired in a glass of diethyl ether / isopentane / ethanol (2:2:1 v/v) in 4 mm diameter quartz tubes using a quartz Dewar.

Luminescence lifetimes of the complexes in deoxygenated solution and at 77K were measured by multichannel scaling (MCS) following excitation of the sample using a pulsed xenon lamp. The emission was detected at 90° to the excitation source, after passage through a monochromator, using a Peltier-cooled R928. The lifetimes in air-equilibrated solution – too short for measurement by MCS – were measured using the same detector operating in time-correlated single-photon counting (TCSPC) mode, using a pulsed laser diode as the excitation source (405 nm excitation, pulse length of 60 ps).

Acknowledgements

We thank Durham University for support of this work. We are grateful to Dr A. S. Batsanov and Dr H. A. Sparkes for crystal structure determination of compounds **d8qb** and **PtL³Cl**, respectively.

Conflicts of Interest

The authors have no conflicts of interest to declare.

Supplementary Material

Crystallographic data for the structure have been deposited with the Cambridge Crystallographic Data Centre as supplementary publication CCDC 2085961–2085964.

References

- [1] (a) D. R. McMillin, J. J. Moore, *Coord. Chem. Rev.* 229 (2002) 113. (b) J. A. G. Williams, S. Develay, D. L. Rochester, L. Murphy, *Coord. Chem. Rev.* 252 (2008) 2596. (c) R. McGuire, M. C. McGuire, D. R. McMillin, *Coord. Chem. Rev.* 254 (2010) 2574. (d) L. Murphy, J. A. G. Williams, *Top. Organomet. Chem.* 28 (2010) 75. (e) Y. Chi, P. T. Chou, *Chem. Soc. Rev.* **39** (2010) 638. (f) A. Diez, E. Lalinde and M. T. Moreno, *Coord. Chem. Rev.* 255 (2011) 2426. (g) K. Li, G. S. M. Tong, Q. Y. Wan, G. Cheng, W. Y. Tong, W. H. Ang, W. L. Kwong, C.M. Che, *Chem. Sci.* 7 (2016) 1653. (h) V. W. W. Yam, A. S. Y. Law, *Coord. Chem. Rev.* 414 (2020) 213298.
- [2] (a) H. Yersin, A. F. Rausch, R. Czerwieniec, T. Hofbeck, T. Fischer, *Coord. Chem. Rev.*, 255 (2011) 2622. (b) P. T. Chou, Y. Chi, M. W. Chung, C. C. Lin, 255 (2011) 2653.
- [3] Y. Chi, P. T. Chou, *Chem. Soc. Rev.* 39 (2010) 638.
- [4] (a) V. Adamovich, J. Brooks, A. Tamayo, A. M. Alexander, P. I. Djurovich, B. W. D'Andrade, C. Adachi, S. R. Forrest, M. E. Thompson, *New J. Chem.* 26 (2002) 1171. (b) M. Cocchi, J. Kalinowski, V. Fattori, J. A. G. Williams, L. Murphy, *Appl. Phys. Lett.* 94 (2009) 073309. (c) W. Mroz, C. Botta, U. Giovanella, E. Rossi, A. Colombo, C. Dragonetti, D. Roberto, R. Ugo, A. Valore, J. A. G. Williams, *J. Mater. Chem.*, 21 (2011) 8653. (d) E. Rossi, A. Colombo, C. Dragonetti, D. Roberto, F. Demartin, M. Cocchi, P. Brulatti, V. Fattori, J. A. G. Williams, *Chem. Commun.* 48 (2012) 3182. (e) Y. C. Wei, S. F. Wang, Y. Hu. L. S. Liao, D. G. Chen, K. H. Chang, C. W. Wang, S. H. Liu, W. H. Chan, J. L. Liao, W. Y. Hung, T. H. Wang, P. T. Chen, H. F. Hsu, Y. Chi, P. T. Chou, *Nat. Photonics.* 14 (2020) 570.
- [5] Q. Zhao, F. Li, C. Huang, *Chem. Soc. Rev.* 39 (2010) 3007.
- [6] (a) V. Fernandez-Moreira, F. L. Thorp-Greenwood, M. P. Coogan, *Chem. Commun.* 46 (2010) 186. (b) K. K. W. Lo, S. P. Y. Li, K. Y. Zhang, *New J. Chem.* 35 (2011) 265. (c) Q. Zhao, C. Huang, F. Li, *Chem. Soc. Rev.* 40 (2011) 2508. (d) E. Baggaley, J. A. Weinstein, J. A. G. Williams, *Coord. Chem. Rev.* 256 (2012) 1762. (e) E. Baggaley, J. A. Weinstein, J. A. G. Williams, *Struct. Bond.* 165 (2015) 205.
- [7] (a) W. Y. Wong and C.L. Ho, *Chem. Soc. Rev.* 253 (2009) 1709. (b) J. Kalinowski, V. Fattori, M. Cocchi, J.A.G. Williams, *Coord. Chem. Rev.* 255 (2011) 2401. (c) C. M. Che, C.C. Kwok, S.W. Lai, A.F. Rausch, W. J. Finkenzeller, N. Y. Zhu, H. Yersin,

-
- Chem. Eur. J. 16 (2010) 233. (d) L. F. Gildea, J. A. G. Williams, "Iridium and platinum complexes for OLEDs", in "Organic Light-Emitting Diodes: Materials, Devices and Applications", ed. A. Buckley, Woodhead, Cambridge, 2013. (e) S. Q. Huo, J. Carroll, D. A. K. Vezzu, Asian J. Org. Chem. 4 (2015) 1210. (f) C. Cebrian, M. Mauro, Beilstein J. Org. Chem. 14 (2018) 1459.
- [8] (a) J. Brooks, Y. Babayan, S. Lamansky, P. I. Djurovich, I. Tsyba, R. Bau, M. E. Thompson, Inorg. Chem. 41 (2002) 3055. (b) P. I. Djurovich, D. Murphy, M. E. Thompson, B. Hernandez, R. Gao, P. L. Hunt, M. Selke, Dalton Trans. 2007, 3763. (c) M. Spencer, A. Santoro, G. R. Freeman, Á. Díez, P. R. Murray, J. Torroba, A. C. Whitwood, L. J. Yellowlees, J. A. G. Williams, D. W. Bruce, Dalton Trans. 41 (2012) 14244. (d) X. Yang, Z. Huang, J. Dang, C.-L. Ho, G. Zhou, W.-Y. Wong, Chem. Commun. 49 (2013) 4406. (e) X. Li, Y. Liu, J. Luo, Z. Zhang, D. Shi, Q. Chen, Y. Wang, J. He, J. Li, G. Lei, Dalton Trans. 41 (2012) 2972. (f) J. R. Berenguer, Á. Díez, A. García, E. Lalinde, M. T. Moreno, S. Sánchez and J. Torroba, Organometallics, 30 (2011) 1646.
- [9] J. A. G. Williams, Top. Curr. Chem. 281 (2007) 205
- [10] (a) S.-W. Lai, M. C.-W. Chan, T.-C. Cheung, S.-M. Peng, C.-M. Che, Inorg. Chem. 38 (1999) 4046. (b) V. W. W. Yam, R. P. L. Tang, K. M. C. Wong, X. X. Lu, K. K. Cheung, N. Y. Zhu, Chem. Eur. J. 8 (2002) 4066. (c) W. Lu, B.-X. Mi, M. C. W. Chan, Z. Hui, C.-M. Che, N. Zhu and S.-T. Lee, J. Am. Chem. Soc. 126 (2004) 4958. (d) P. H. Lanoë, J. L. Fillaut, L. Toupet, J. A. G. Williams, H. Le Bozec, V. Guerchais, Chem. Commun. 36 (2008) 4333. (e) J. Moussa, K. Haddouche, L. M. Chamoreau, H. Amori, J. A. G. Williams, Dalton Trans. 45 (2016) 12644.
- [11] (a) J. A. G. Williams, A. Beeby, E. S. Davies, J. A. Weinstein, C. Wilson, Inorg. Chem. 42 (2003) 8609. (b) S. J. Farley, D. L. Rochester, A. L. Thompson, J. A. K. Howard, J. A. G. Williams, Inorg. Chem. 44 (2005) 9690. (c) W. L. Tong, M. C. W. Chan, S. M. Yiu, Organometallics, 29 (2010) 6377. (d) S.-L. Lai, W.-Y. Tong, S. C. F. Kui, M.-Y. Chan, C.-C. Kwok, C.-M. Che, Adv. Funct. Mater. 23 (2013) 5168. (e) W. A. Tarran, G. R. Freeman, L. Murphy, A. M. Benham, R. Katakay, J. A. G. Williams, Inorg. Chem. 53 (2014) 5738.
- [12] (a) A. Rausch, L. Murphy, J. A. G. Williams, H. Yersin, Inorg. Chem. 48 (2009) 11407. (b) A. Rausch, L. Murphy, J. A. G. Williams, H. Yersin, Inorg. Chem. 51 (2012) 312.

-
- [13] (a) R. Englman, J. Jortner, *Mol. Phys.* 18 (1970) 145. (b) E. M. Kober, J. V. Caspar, R. S. Lumpkin, T. J. Meyer, *J. Phys. Chem.* 90 (1986) 3722.
- [14] (a) R. Weissleder, V. Ntziachristos, *Nat. Med.* 9 (2003) 123. (b) W.R. Zipfel, R.M. Williams, W.W. Webb, *Nat. Biotechnol.* 21 (2003) 1368.
- [15] (a) A. Aliprandi, D. Genovese, M. Mauro, L. De Cola, *Chem. Lett.* 44 (2015) 1152. (b) K. T. Li, R. W. Chen-Cheng, H. W. Lin, Y. J. Shiau, S. H. Liu, P. T. Chou, C. S. Tsao, Y. C. Huang, Y. Chi, *Nat. Photonics* 11 (2017) 63. (c) E. V. Puttock, M. T. Walden, J. A. G. Williams, *Coord. Chem. Rev.* 367 (2018) 127. (d) E. Garoni, J. Boixel, V. Dorcet, T. Roisnel, D. Roberto, D. Jacquemin, V. Guerschais, *Dalton Trans.* 47 (2018) 224. (e) C. L. Ko, W. Y. Hung, P. T. Chen, T. H. Wang, H. F. Hsu, J. L. Liao, K. T. Ly, S. F. Wang, C. H. Yu, S. H. Liu, G. H. Lee, W. S. Tai, P. T. Chou, Y. Chi, *ACS Appl. Mater. Interfaces* 12 (2020) 16679. (f) S. F. Wang, Y. Yuan, Y. C. Wei, W. H. Chan, L. W. Fu, B. K. Su, I. Y. Chen, K. J. Chou, P. T. Chen, H. F. Hsu, C. L. Ko, W. Y. Hung, C. S. Lee, P. T. Chou, Y. Chi, *Adv. Funct. Mater.* 30 (2020) 2002173.
- [16] (a) M. A. Baldo, D. F. O'Brien, Y. You, A. Shoustikov, S. Sibley, M. E. Thompson, S. R. Forrest, *Nature* 395 (1998) 151. (b) K. R. Graham, Y. X. Yang, J. R. Sommer, A. H. Shelton, K. S. Schanze, J. G. Xue, J. R. Reynolds, *Chem. Mater.* 23 (2011) 5305. (c) C. O. Paul-Roth, S. Drouet, A. Merhi, J. A. G. Williams, L. F. Gildea, C. Pearson, M. C. Petty, *Tetrahedron* 69 (2013) 9625.
- [17] (a) P. Mandapati, J. D. Braun, C. Killeen, R. L. Davis, J. A. G. Williams, D. E. Herbert, *Inorg. Chem.* 58 (2019) 14808. (b) P. Mandapati, J. D. Braun, I. B. Lozada, J. A. G. Williams, D. E. Herbert, *Inorg. Chem.* 59 (2020) 12504
- [18] K. J. H. Young, X. Bu, W. C. Kaska, *J. Organomet. Chem.* 696 (2011) 3992.
- [19] (a) H. Wolpher, O. Johansson, M. Abrahamsson, M. Kritikos, L. Sun, B. Akermark, *Inorg. Chem. Commun.* 7 (2004) 337. (b) Y. Hu, M. H. Wilson, R. Zong, C. Bonnefous, D. R. McMillin, R. P. Thummel, *Dalton Trans.* (2005) 354. (c) M. Abrahamsson, M. Jäger, T. Österman, L. Eriksson, P. Persson, H. Becker, O. Johansson, L. Hammarström, *J. Am. Chem. Soc.* 128 (2006) 12616. (d) A. W. Garner, C. F. Harris, D. A. K. Vezzu, R. D. Pike, S. Huo, *Chem. Commun.* 47 (2011) 1902. (e) D. A. K. Vezzu, D. Ravindranathan, A. W. Garner, L. Bartolotti, M. E. Smith, P. D. Boyle, S. Huo, *Inorg. Chem.* 50 (2011) 8261.
- [20] K. L. Garner, L. F. Parkes, J. D. Piper and J. A. G. Williams, *Inorg. Chem.* 49 (2010) 476.

-
- [21] J. Hu, H. Xu, M.-H. Nguyen, J. H. K. Yip, *Inorg. Chem.* 48 (2009) 9684.
- [22] (a) W. Sotoyama, T. Satoh, H. Sato, A. Matsuura, N. Sawatari, *J. Phys. Chem. A*, 109 (2005) 9760. (b) D. L. Rochester, S. Develay, S. Zális, J. A. G. Williams, *Dalton Trans.* (2009) 1728.
- [23] M. Z. Shafikov, P. Pander, A. V. Zaytsev, R. Daniels, R. Martinscroft, F. B. Dias, J. A. G. Williams, V. N. Kozhevnikov, *J. Mater. Chem.* 9 (2021) 127.
- [24] G. R. Freeman, J. A. G. Williams *Top. Organomet. Chem.* 40 (2013) 89.
- [25] (a) K. Nakamaru, *Bull. Chem. Soc. Jpn* 55 (1982) 2697. (b) A. Juris, V. Balzani, P. Belser, A. Von Zelewsky, *Helv. Chim. Acta* 64 (1981) 2175.
- [26] H. Ghaieni, M. Sharifi, M. Fattolahy, *Dyes Pigm.* 72 (2007) 97.
- [27]. C. J. Aspley, J. A. G. Williams, *New J. Chem.* 25 (2001) 1136.
- [28] O. V. Dolomanov, L. J. Bourhis, R. J. Gildea, J. A. K. Howard and H. Puschmann, *J. Appl. Cryst.* (2009), **42**, 339-341
- [29] G.M. Sheldrick, *Acta Cryst.* (2008), **A64**, 112-122
- [30] K. Suzuki, A. Kobayashi, S. Kaneko, K. Takehira, T. Yoshihara, H. Ishida, Y. Shiina, S. Oishi, S. Tobita, *Phys. Chem. Chem. Phys.* 11 (2009) 9850.